

Road Gradient Estimation Using Smartphones: Towards Accurate Estimation on Fuel Consumption and Air Pollution Emission on Roads

Liuwang Kang
University of Virginia, USA
Email: lk2sa@virginia.edu

Haiying Shen
University of Virginia, USA
Email: hs6ms@virginia.edu

Zhuozhao Li
University of Chicago, USA
Email: zhuozhao@uchicago.edu

Abstract—Accurate estimations on vehicle fuel consumption and pollution emission on roads are important for vehicle velocity optimization and driving route planning. Existing methods for such estimations only consider vehicle driving speed and acceleration but neglect the influence of road gradient. This is mainly because the road gradients for most road networks are not available and none of existing methods for road gradient estimation can be conducted inexpensively in practice and keep high road gradient estimation accuracy simultaneously. Thus, how to estimate the road gradient conveniently and accurately is an important but challenging problem. To handle this challenge, we propose a new road gradient estimation system which estimates the road gradient only using a smartphone. When a vehicle is driving, a smartphone in the vehicle continuously measures vehicle states (velocity, acceleration, steering rate, position), which are used to estimate the road gradient. To eliminate measuring noise and drift noise, the deviation between the measured value and estimated value is used to adjust the estimated value. Since measured vehicle states when a vehicle changes lane adversely influence the accuracy of road gradient estimation, we design lane change detection to eliminate such influences. Finally, given a group of road gradient estimates for a given route, we use the track fusion algorithm to further eliminate measuring noise and drift noise and improve road gradient estimation accuracy. We conducted driving experiments in a city area to evaluate our system. The experimental results show that our system's estimation error is reduced by 22% compared with existing methods. The results also demonstrate the accuracy of our lane change detection. Finally, we integrated the road gradient values into vehicle fuel consumption and air pollution emission model to estimate fuel consumption and air pollution emission and found that the estimation values increase by 33.4% compared with the values without considering road gradient.

I. INTRODUCTION

Vehicle popularization in the world has resulted in some problems such as fuel shortage and air pollution. In order to save fuel consumption and protect the environment, it is important to model fuel consumption and carbon dioxide emissions [1] for the estimation. A number of studies have highlighted the significant effects of the road gradient on the vehicle fuel consumption and air pollution emission. Frey *et al.* [2] showed that vehicle fuel consumption can increase by 40% when the road gradient changes from 0° to 5° . Boriboonsomsin *et al.* [3] demonstrated that compared with a flat route, the vehicle driving on a downhill route reduces the fuel consumption by 2 times while the fuel consumption increases by 1.5 to 2 times for an uphill route. Therefore,

estimating road gradient and applying it into fuel consumption and air pollution emission models becomes necessary.

As one of the most powerful web maps, Google Maps provides street maps, real-time traffic conditions and road gradient for users. However, its road gradient is only for roads used by walkers and bicyclers [4] and its road gradient information shows no accurate road gradient values but only basic trendlines. Google Maps does not provide road gradient information for vehicle driving roads, perhaps because it does not directly affect the driving experience. However, it affects the vehicle fuel consumption and hence final driving route planning, especially for the roads with large road gradient.

Though many efforts have been devoted to estimating the road gradient, none of them can be conducted inexpensively in practice and keep high road gradient estimation accuracy simultaneously. Some methods [5], [6], [7], [8] estimate road gradient based on vehicle states including vehicle mass, engine torque, active gear, vehicle speed and position. The studies in [5], [6] assume that the active gear keeps the same during the driving process though it is changed frequently in practice and difficult to measure in real time. To deal with such a problem, [7], [8] tried to measure real-time active gear values using the gearbox management system, which is only available in premium cars. Besides, these methods do not consider lane change actions, which may result in road gradient estimation errors (we will explain the details later). Other methods [9], [10], [11] estimate the road gradient by placing the articulated wheeled profilograph machine behind the frontal vehicle and moving the profilograph machine over the road. The profilograph machine is driven by frontal vehicle and needs special setup in advance for different road types, which makes them expensive to implement. Besides, they have high requirements on sensor accuracy and signal processing speed during the operation. Then, a challenge is how to estimate road gradient of a road network accurately and inexpensively.

A smartphone has powerful embedded sensors and can provide users different auxiliary functions. Considering the popularity of smartphones, we propose a smartphone-based system to estimate the road gradient of driving roads and apply the road gradient values into the fuel consumption and pollution emission model. Our proposed system uses a smartphone in a driving vehicle to measure vehicle's driving states (including vehicle velocity, acceleration, steering rate

and position) for the road gradient estimation. We build a vehicle state space equation that can calculate road gradient at a location based on vehicle longitudinal velocity and acceleration. Since the measuring noise and drift noise exist in the measurement data from the smartphone, we apply Extended Kalman Filter (EKF) to eliminate the effect of measuring noise and drift noise on road gradient estimation accuracy based on the deviation between estimated vehicle velocity and measured vehicle velocity. Finally, given a group of road gradient estimates (calculated from different velocity measures by different sensors in a smartphone and CAN-bus (by connecting the smartphone to CAN-bus through bluetooth)), for a given route, we use track fusion algorithm [12] to eliminate measuring noise and drift noise and improve road gradient estimation accuracy.

To the best of our knowledge, it is the first work to estimate the road gradient using a smartphone, and consider the road gradient effects on estimating fuel consumption and pollution emission in practice. However, there exist one challenge in estimating the road gradient with the smartphone in practice (that are neglected in previous approaches). Drivers usually conduct lane change actions frequently. During the lane change process, the longitudinal velocity does not equal to the measured vehicle velocity. Road gradient estimation error occurs if the measured vehicle velocity is directly used as the longitudinal velocity to estimate the road gradient. Current steering assistance system helps to detect driver's lane change action based on advanced built-in sensors (e.g., cameras, infrared sensor and radars) that only exist in premium cars, which limits its wide application nowadays in practice. Therefore, the challenge is to detect lane change actions only using a smartphone and eliminate the influence of lane change actions on the road gradient estimation accuracy. For this challenge, we propose lane change detection algorithm to detect lane change actions during the driving process and eliminate its effect on road gradient estimation by adjusting the vehicle states.

To verify the road gradient estimation system, we conducted driving experiments in the city area of Charlottesville, VA. In the driving experiments, we conducted road gradient estimation comparison between our proposed system and existing methods. Our contributions are summarized below:

- We propose a road gradient estimation system which uses a smartphone in a driving vehicle to measure the vehicle's driving states to estimate the road gradient. More specifically, we build vehicle state space equation to estimate the road gradient based on vehicle states, and apply the EKF algorithm and track fusion algorithm to eliminate the measuring noise and drift noise and improve road gradient estimation accuracy.
- To improve vehicle state online measurement accuracy (and hence the accuracy of road gradient estimation), we propose lane change detection algorithm. Lane change detection algorithm detects lane change actions during driving process and calculates longitudinal velocity from the measured velocity.
- We conduct driving experiments in the city area of Charlottesville to verify our system. The results demonstrate the effectiveness of lane change detection algorithm. They also

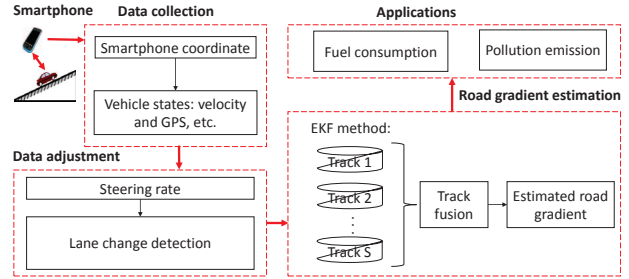


Fig. 1. The framework of road gradient estimation system.

show that our proposed system's estimation error is reduced by 22% compared with existing road gradient estimation methods. In addition, we integrate road gradient values into fuel consumption and pollution emission model to estimate fuel consumption and pollution emission. When road gradient is considered, fuel consumption and pollution emission estimation values increase by 33.4% compared with the values without considering road gradient.

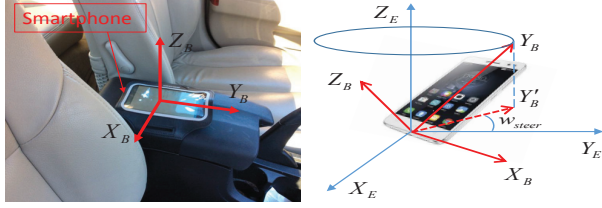
The rest of this paper is organized as follows. Section II presents an overview of our proposed road gradient estimation system. We present the details of the system in Section III and evaluate our system in Section IV. Section V presents related research work. Finally, we conclude this paper in Section VI.

II. SYSTEM FRAMEWORK

Figure 1 presents the framework of our proposed road gradient estimation system. The system contains four major parts: data collection, data adjustment, road gradient estimation and applications. In the data collection part, the smartphone coordinate alignment system is built to describe the relative location between the smartphone and the vehicle and calculate the vehicle steering rate. The data adjustment part includes lane change detection algorithm. Lane change detection algorithm detects possible lane change actions based on vehicle steering rate, which is the change of the angle (between vehicle driving direction and road direction) per second. If the lane change action is detected, vehicle longitudinal velocity during the lane change process is derived from the measured vehicle velocity to eliminate lane change's adverse effect on road gradient estimation accuracy. In the road gradient estimation part, measuring vehicle states are used to estimate the road gradient using the vehicle state space equation and EKF. Since vehicle velocity can be obtained through different ways such as speedometer, GPS data and accelerometer in the measuring process, it will result in different possible road gradient estimation tracks (series of estimation values). Different vehicles also get different road gradient estimation tracks for the same road. Here, track fusion algorithm is adopted to fuse the road gradient estimation tracks in order to improve the road gradient estimation accuracy.

III. SYSTEM DESIGN

In this section, we present how to build smartphone coordinate alignment system for data collection. Then, we propose lane change detection algorithm and road gradient estimation method to estimate road gradient based on measured data.



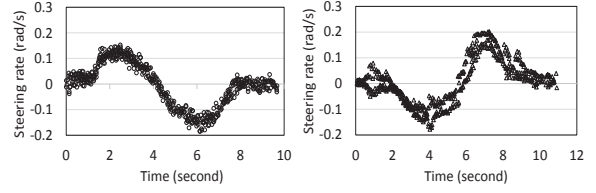
(a) Smartphone in the vehicle (b) Coordinate alignment
Fig. 2. Smartphone coordinate alignment.

A. Data Collection

In the road gradient estimation system, the smartphone is put in the vehicle and sensors in the smartphone are used to collect vehicle driving states for the road gradient estimation. The measured vehicle states contain vehicle velocity, vehicle acceleration, vehicle steering rate and vehicle position (latitude and longitude). A smartphone has different built-in sensors [13] to measure these parameters. The accelerometer and speedometer can be used to measure vehicle acceleration and velocity, respectively. GPS data in the smartphone shows vehicle position and its value is updated per second. The vehicle steering rate can not be directly measured and we calculate it based on road direction change rate (w_{road}) and vehicle driving direction change rate ($\hat{w}_{vehicle}$) that can be measured with angular velocity sensor.

In the smartphone coordinate system $X_B Y_B Z_B$, as shown in Figure 2(a), Z_B represents the direction that is vertical to the surface of the smartphone, X_B and Y_B represent other two directions that are parallel to the surface of the smartphone. The speedometer and accelerometer in the smartphone measure the smartphone velocity and acceleration in the smartphone coordinate system $X_B Y_B Z_B$. Note that we need vehicle longitudinal velocity to estimate road gradient. To ensure that the smartphone's measured velocity in the Y_B direction equals to the vehicle velocity, we align the smartphone coordinate system $X_B Y_B Z_B$ with the road coordinate system $X_E Y_E Z_E$ to form the smartphone coordinate alignment system; that is, the smartphone is faced up and its Y_B direction is the same as the vehicle driving direction as shown in Figure 2(a). The smartphone is kept at the same location in the vehicle without any relative movement, so it is assumed that the smartphone and the vehicle would always have same moving states (velocity, acceleration and steering angle).

The vehicle driving direction change rate $\hat{w}_{vehicle}$ is the rate of angle change between vehicle driving direction and earth East direction. The road direction change rate w_{road} is the rate of angle change between road direction and earth East direction. In the smartphone coordinate alignment system, the vehicle driving direction change rate $\hat{w}_{vehicle}$ can be described as the rotation rate of plane $X_B Y_B$ around Z_B axis and the road direction change rate w_{road} can be described as the rotation rate of plane $X_E Y_E$ around Z_E axis, which can be calculated based on road geography information (longitude and latitude). The angular velocity sensor in the smartphone measures the vehicle driving direction change rate $\hat{w}_{vehicle}$. It equals to the sum of vehicle steering rate w_{steer} and the road



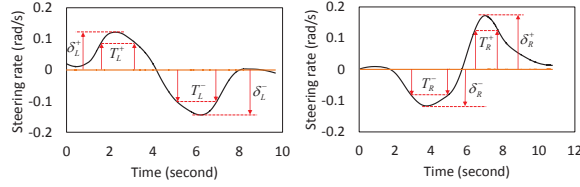
(a) Left lane change (b) Right lane change
Fig. 3. Steering rate when the vehicle makes left/right lane change.

direction change rate w_{road} : $\hat{w}_{vehicle} = w_{steer} + w_{road}$. Thus, vehicle steering rate (needed for estimating road gradient) is calculated by $w_{steer} = \hat{w}_{vehicle} - w_{road}$. To show the vehicle steering rate w_{steer} clearly, as shown in Figure 2(b), we project Y_B axis on the $X_E - Y_E$ plane to get the new axis Y'_B . The angle change rate between Y_E axis and Y'_B axis is vehicle steering rate w_{steer} and can be calculated as $\hat{w}_{vehicle} - w_{road}$. Note that the smartphone coordinate system and the road coordinate system may not be aligned in some situations such as smartphone's relevant movements when the vehicle starts or stops. These relevant movements will affect steering rate measurement accuracy of the smartphone coordinate alignment system. Here, we use the method in [14] to eliminate the effects of smartphone's relevant movements on the smartphone coordinate alignment system.

B. Lane Change Detection

When a vehicle drives on the road, the vehicle always conducts frequent steering actions. Based on the lane change study [15], the average lane change numbers per mile is around 0.36. In addition, the lane change frequency in the urban area is much larger than the value in the highway. When the vehicle drives along the road, the longitudinal velocity equals to measured vehicle velocity from the smartphone or CAN-bus. During the lane change process, the longitudinal velocity can not be represented by the measured vehicle velocity. If the measured vehicle velocity is directly used for the road gradient estimation during lane change process, it will cause a large road gradient estimation error. To eliminate effects of lane change, we firstly detect when the lane change action starts based on vehicle states. Then, the vehicle steering angle during the lane change process needs to be figured out. Finally, the vehicle longitudinal velocity is adjusted based on steering angle to estimate road gradient.

1) *Lane change feature extraction:* We know that during the left lane change, the steering wheel firstly experiences a counter-clockwise rotation and then a clockwise rotation, which corresponds to the positive and then negative values in the smartphone coordinate system. Oppositely, the right lane change produces negative and then positive values in the smartphone coordinate system. We did vehicle steering experiments with ten drivers and measured their average steering rates during the lane change process. In the experiments the driving speed range is between 15km/h and 65km/h and the average steering rates during left and right lane changes are shown in Figure 3.



(a) Left lane change feature (b) Right lane change feature

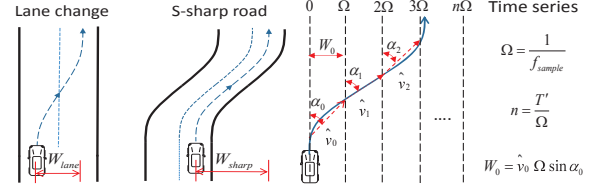
Fig. 4. Feature extraction of steering rate with different driving maneuvers.

In Figure 3, we see that the steering rate experiences both positive and negative bumps in both a left lane change and a right lane change. For the left lane change, the positive bump is followed by the negative bump. For the right lane change, opposite situation occurs. To show the steering rate dynamics more clearly, we applied the local regression method [16] to filter measuring noise and drift noise in the steering rate data and smooth the steering rate profile. The smoothed steering rate profiles during the left and right lane change processes are shown in Figure 4. Here we define two parameters (δ and T) to describe bump features. δ is the maximum absolute magnitude in the steering rate profile and used to describe the strength level of steering rate. T represents the time duration of the steering rate above certain high strength level (i.e., 0.7δ). Here, the threshold value is assigned to be 0.7δ because this threshold value can effectively eliminate the effects of angular velocity sensor measuring noise and drift noise and road driving condition on bump detection accuracy in the vehicle steering experiments. In practice its coefficient can be adjusted based on the value of steering angle noises led by vehicle tire condition and road roughness [17]. We identify two corresponding necessary conditions to detect possible bumps in a steering rate profile. One condition is that the maximum absolute magnitude of the steering rate profile should be not less than δ and the other condition is that the time duration of the steering angle varying between 0.7δ and δ should be more than T .

TABLE I
EXTRACTED FEATURES OF THE BUMP.

δ_L^+	δ_L^-	δ_R^+	δ_R^-	Minimum value (rad/s)
0.1215	0.1445	0.1723	0.1167	0.1167
T_L^+	T_L^-	T_R^+	T_R^-	Minimum value (second)
1.625	1.766	1.383	2.072	1.383

For left lane change shown in Figure 4(a), δ_L^+ and δ_L^- are maximum magnitudes of positive bump and negative bump, respectively. T_L^+ and T_L^- are corresponding time durations. Similarly, the parameter definitions of δ_R^+ , δ_R^- , T_R^+ and T_R^- are applicable to right lane change situation. Since there is collected data for many left/right turns from one or many vehicles, we assign δ and T the minimum values among maximum absolute magnitudes and time durations during left and right lane changes in order not to miss any bumps whose features are close to our results. For example, to figure out δ and T which are used to detect both left and right lane changes, we compared steering rate data of 10 drivers under different lane change processes. The comparison results are



(a) Steering track comparison (b) Horizontal displacement

Fig. 5. Horizontal displacement for lane change detection.

shown in Table I and δ and T are 0.1167rad/s and 1.383s .

2) *Lane change detection*: In the above section, we extracted the lane change features based on the steering experiments. When the vehicle drives on the road, we calculate the vehicle steering rate through the method introduced in Section III-A and record it as steering rate profile. We check possible bumps in the steering rate profile with bump features and detect possible bumps by comparing two neighboring bumps (positive or negative) in the profile. However, when the vehicle passes through the S-sharp road, it will also produce similar negative and positive bumps. Figure 5(a) shows the vehicle steering track comparisons between right lane change and S-sharp road. Therefore, we should consider how to distinguish whether a vehicle is conducting lane change from driving along a S-sharp road and avoid wrong lane change detection.

In general, the average horizontal displacement W_{lane} is around 3.65m after making the lane change while the average horizontal displacement W_{sharp} for a S-sharp road is usually much larger than W_{lane} [18]. Here, we use the horizontal displacement of bumps to distinguish lane change action and S-sharp road. For the horizontal displacement of the bump which is less than $3W_{lane}$ [15], we consider it as the lane change action rather than S-sharp road. Figure 5(b) shows how the horizontal displacement is calculated during the whole right lane change process. As shown in right part of Figure 5(b), f_{sample} is the smartphone sampling frequency and Ω is the time period per each data measurement. T' is total time of the lane change process and the steering angle α_i at i^{th} time period equals to $\sum_{j=0}^i (w_{steer}^j \Omega)$. w_{steer}^j represents the steering rate w_{steer} at the j^{th} time period which can be measured through the smartphone coordinate alignment system in Section III-A. Therefore, horizontal displacement W during lane change process can be calculated as Equation (1).

Based on the above lane change feature extraction and horizontal displacement calculation, we propose the lane change detection algorithm to detect possible lane change actions shown as Algorithm 1. The algorithm firstly detects possible bumps based on the measured steering rate and recorded bump status during the trip. *Line 1* find outs possible bumps which satisfy the bump feature requirements. *Line 4* checks the state of possible bumps in the steering rate profile. If one possible bump is detected and the bump status is *no-bump*, the bump status will be assigned as *one-bump* and its type (positive or negative) will be recorded. Otherwise, the algorithm will skip to *Line 8* and compare types between the bump and its neighbor bump. If the bump type is the same to neighbor bump type, the algorithm will skip to *Line 13* directly and continue

next detection loop. If the bump and its neighbour bump have opposite types and horizontal displacement is less than $3W_{lane}$ [15], we can conclude that the vehicle has the lane change and the algorithm will go to *Line 10* to determine the lane change type.

$$W = \sum_{i=0}^n \hat{v}_i \Omega \sin\left(\sum_{j=0}^i w_{steer}^j \Omega\right) \quad (1)$$

Where n is the number of time periods during the lane change process; \hat{v}_i and α_i represent the vehicle velocity and steering angle at i^{th} time period, respectively.

Algorithm 1: Lane change detection algorithm

Data: Steering rate w_{steer} and bump status are known
1 Calculate the maximum magnitude $|w_{steer}|$ and time duration T_1 of w_{steer} varying between $0.7|w_{steer}|$ and $|w_{steer}|$;
2 **while** $|w_{steer}| \geq \delta$ and $T_1 \geq T$ **do**
3 Possible bump is detected and its sign is recorded;
4 **if** STATE is *no-bump* **then**
5 STATE becomes *one-bump*;
6 Its bump sign is recorded;
7 **else**
8 Check the sign between two bumps to decide whether their signs are opposite;
9 **if** the signs are opposite and $W \leq 3W_{lane}$ **then**
10 Determine lane change type based on signs;
11 STATE becomes *no-bump*;
12 **else**
13 Do nothing and continue;
14 **end**
15 **end**
16 **end**

3) *Lane change effect elimination:* After lane change actions are determined with lane change detection algorithm, the vehicle longitudinal velocity during the lane change process needs to be adjusted for high road gradient estimation accuracy. The vehicle velocity in the longitudinal direction can be adjusted through Equation (2).

$$\hat{v}_i^L = \hat{v}_i \cos\left(\sum_{j=0}^i w_{steer}^j \Omega\right) \quad (2)$$

Where \hat{v}_i^L represents the vehicle longitudinal velocity at the i^{th} time period. Since the vehicle longitudinal velocity will be adjusted through Equation (2) for every lane change process, the effects of possible lane change actions on road gradient can be eliminated effectively.

C. Road Gradient Estimation

1) *Vehicle driving equation:* Although the barometer in the smartphone can be used to measure the altitude, its accuracy is notoriously poor (e.g., several meters) [19] in practice. Because of the limit of barometer low accuracy, it is difficult to obtain accurate road gradient estimation even by applying existing noise elimination algorithms such as EKF to eliminate barometer measuring noise and drift noise. Compared with the barometer, the speedometer and accelerometer in the smartphone have high measurement accuracy. Therefore, we build a road gradient estimation equation to estimate the road gradient based on vehicle driving states including velocity and

acceleration, etc. In order to estimate the road gradient with measured vehicle states, the relationship between measured vehicle states and the road gradient needs to be established. We derive the relationship between vehicle states and road gradient θ from [20] as follows:

$$\theta = \arcsin\left(\frac{M}{rmg} - \frac{\rho A_f C_d v^2}{2mg} - \frac{a}{g}\right) - \beta \quad (3)$$

where M is vehicle driving torque and r is wheel radius; m is gross weight; ρ is average air density; A_f is frontal area of the vehicle; C_d is drag coefficient; v is vehicle velocity; a is vehicle acceleration value and g means gravity constant; μ is rolling resistance coefficient and $\beta = \arcsin\left(\frac{\mu}{\sqrt{1+\mu^2}}\right)$ is a constant value (which indicates the rate of rolling resistance to gross weight). Vehicle driving torque M can be calculated based on the engine torque measured through smartphone apps [21]. Since other parameters are constant and known in advance, the road gradient can be calculated with Equation (3). However, the above velocity value contains measuring noise and drift noise during the measurement process, which results in low road gradient estimation accuracy. In the next section, we build the vehicle state space equation to describe road gradient dynamics and integrate it with EKF [22] to eliminate effects of measuring noise and drift noise.

2) *Vehicle state space equation:* When the vehicle drives on the road, the dynamics of road gradient θ can be shown as Equation (4):

$$\dot{\theta} = \frac{\rho A_f C_d v a}{mg \cos \theta} \quad (4)$$

here, Equation (4) is derived by taking the derivative of Equation (3). When the vehicle drives on the road with road gradients, rolling resistance (which corresponds to β in Equation (3)) is much smaller than other resistances such as road gradient resistance (which is related to θ) and acceleration resistance (which is related to a). Therefore, we ignore the rolling resistance during the derivation process. Since the data measured through the smartphone is digital value, we change Equation (4) into discrete form through first order Euler approximation to generate discrete-time vehicle state space equation shown as follows:

$$\begin{bmatrix} v(t+1) \\ \theta(t+1) \end{bmatrix} = \begin{bmatrix} v(t) + \hat{a}(t) \\ \theta(t) + \frac{\rho A_f C_d v(t) \hat{a}(t)}{mg \cos \theta(t)} \end{bmatrix} \quad (5)$$

where t denotes the discrete time sample number; $v(t)$ and $\theta(t)$ are defined as estimated longitudinal velocity and road gradient at time t ; $\hat{a}(t)$ is measured vehicle longitudinal acceleration value. As explained in Section III-C1, parameters ρ , A_f , C_d , m and g are constant values and there is no need to measure them. The measured longitudinal acceleration $\hat{a}(t)$ contains noises, which can result in road gradient estimation error by Equation (5). To eliminate the effects of such noises on road gradient estimation accuracy, we use EKF to eliminate noises and finally determine longitudinal velocity and road gradient. EKF is an algorithm for non-linear systems, which utilizes a series of measurements containing noises to estimate

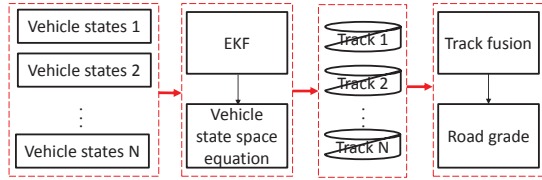


Fig. 6. Track fusion algorithm for road gradient estimation.

unknown variables that tend to be more accurate than those estimated based on a single measurement alone.

We use $\hat{v}(t+1)$ to denote measured longitudinal velocity from the smartphone or CAN-bus at time $t+1$. EKF updates vehicle velocity and road gradient with their previous state values and eliminates the negative effect of noises by adjusting its Kalman gain matrix K during each update process. The matrix $[v(t+1), \theta(t+1)]$ is firstly estimated based on matrix $[v(t), \theta(t)]$ and Equation (5) and denoted as matrix $[v(t+1|t), \theta(t+1|t)]$. Then, Kalman gain matrix K is adjusted in the calculation process based on the velocity deviation $\Delta = \hat{v}(t+1) - v(t+1|t)$ and Equation (5). Finally, the matrix $[v(t+1), \theta(t+1)]$ is adjusted based on K and deviation Δ and it equals to $[v(t+1|t), \theta(t+1|t)] + K\Delta$. More details about how to use EKF to measure a variable with the consideration of the noises can be found in [22].

3) *Track fusion for road gradient estimation:* When the vehicle drives on the road, vehicle velocity can be obtained through different ways such as GPS data, speedometer and accelerometer. The above methods usually generate different velocity values for the same vehicle, which results in different road gradient estimation tracks. Different vehicles also generate different road gradient estimation tracks for a given road. To get the final road gradient estimation, we use the track fusion algorithm [23] to fuse these estimated road gradient tracks. By the track fusion algorithm, we can take full advantages of these velocity measurements and obtain more accurate road gradient estimation value. Here we develop multi-sensor road gradient estimation system which integrates track fusion and road gradient estimation together to obtain more accurate estimation value.

The multi-sensor road gradient estimation system can be shown as Figure 6. Vehicle states including velocities from different sensors are firstly formed for the road gradient estimation. Then, based on vehicle states, vehicle state space equation and EKF are integrated together to estimate road gradient tracks. Finally, these road gradient tracks are fused together by the track fusion algorithm to improve the estimation accuracy of road gradient. In this paper, each road gradient track belongs to sensor track type and there is no cross covariance between any two road gradient tracks. Therefore, we select basic convex combination algorithm as our track fusion algorithm for its simple implementation and good fusion performance [23]. In the basic convex combination algorithm, different road gradient tracks are linearly combined together. The final road gradient can be calculated by:

$$\bar{\theta} = U \sum_{k=1}^N (P_k^{-1} \theta_k) \quad (6a)$$

$$U = \left(\sum_{k=1}^N P_k^{-1} \right)^{-1} \quad (6b)$$

where $\bar{\theta}$ is the final road gradient estimation value through track fusion; θ_k is the road gradient value for the k^{th} track; N is the number of total tracks; U is the system covariance matrix of N road gradient tracks and used to fuse different road gradient values through Equation (6a). P_k represents estimation error covariance matrix of the k^{th} track in EKF. After a vehicle obtains the road gradient of a road, it can upload it to the cloud and the cloud can use the track fusion algorithm to fuse road gradient results from different vehicles, which produces more accurate road gradient and can be used in transportation services such as routing planning.

D. Reference Road Gradient for Performance Evaluation

To evaluate the performance of our proposed system, we need to know the road gradient ground truth in advance. Here, we design a method to obtain reference road gradient profile based on road geography information including the latitude, the longitude and the altitude. To obtain road gradient ground truth of a certain road, we firstly obtain road altitude information by driving a vehicle installing an altimeter whose measuring accuracy reaches around 0.01 meter and manually divide the road into small equal segments from South to North and from West to East. And then, for each small road segment, its starting point and ending point are marked with S and E respectively. The latitude and longitude of its starting point and ending point are used to infer road segment direction. Here the road segment direction represents the angle of road segment relative to the earth East direction and can be calculated as $\arctan \frac{\lambda_E - \lambda_S}{\varphi_E - \varphi_S}$, where φ_S are λ_S the latitude and longitude of starting point, φ_E and λ_E are for ending point. The altitude difference between starting point and ending point is used to calculate its road gradient of a road segment: $\arcsin \frac{z_E - z_S}{d}$, where z_S and z_E are the altitudes of starting point and ending point, and d is the road segment length. Finally, these small road segments are connected together to form the whole route and their road gradient values constitute the reference road gradient profile. Since precisions of road geography information such as latitude/longitude and altitude can reach at 0.00001 degree level and 0.01 meter level, respectively, this method can calculate the road gradient accurately. However, this method requires high manual measurement load, which limits its application in practice. In contrast, our proposed road gradient estimation system estimates road gradients only using a smartphone and does not have manual measurement load.

E. Fuel Consumption and Pollution Emission Model

The road gradient information can be exploited for estimating fuel consumption and air pollution emission on the road surface level. There exist several models for fuel consumption

estimation, which quantify the relationship between fuel consumption and driving states such as driving velocity, acceleration and road gradient. In this paper, the most frequently used model – Vehicle Specific Power (VSP) [24], [1] is employed to estimate vehicle power per unit mass. By utilizing the vehicle mass and the gasoline gallon equivalent (GGE), we can convert VSP into Equation (7) to calculate fuel consumption per hour Γ under different vehicle velocities and road gradients.

$$\Gamma = \frac{1}{GGE} (Av^3 + Bmv \sin \theta + Cmv + mav + Dma) \quad (7)$$

Where Γ represents vehicle gasoline consumptions per hour (*gallon/hour*) and v is vehicle velocity (*m/s*); m is gross vehicle weight and A , B , C and D are parameter coefficients. The parameters used for fuel consumption estimation in this paper are shown in Table II. Although diversity of vehicles will slightly affect the final computation of fuel consumption, fuel consumption estimation above is still useful because the above consumption calculation of selected passenger car (with average gross vehicle weight $1,479kg$) can represent most vehicles' fuel consumptions.

TABLE II
VEHICLE PARAMETERS FOR PERFORMANCE EVALUATION.

GGE	A	B	C	D	m
0.0545	4.7887	21.2903	0.3925	3.6000	1.479

As for air pollution emissions such as carbon dioxide and PM2.5, the vehicle's emissions are proportional to its fuel consumption. For example, around 8,908g of carbon dioxide are produced from burning a gallon of gasoline. Every gallon of gasoline burned creates about 0.084g of PM2.5. Therefore, we can estimate vehicle emissions based on its fuel consumption through the relationship $m_{emission} = FV_{fuel}$, where $m_{emission}$ and V_{fuel} represent the vehicle emission mass (g) and the consumed fuel volume (gallon), respectively. F is the coefficient between vehicle emission and fuel consumption. For example, it equals to 8,908 for carbon dioxide and 0.084 for PM2.5.

IV. PERFORMANCE EVALUATION

To evaluate the performance of our proposed road gradient estimation system, we conducted the driving experiments in the city of Charlottesville, VA. We put Samsung Galaxy S5 smartphone into Nissan Altima 2006 and drove the vehicle on different roads to collect experimental data. We used the method introduced in Section III-D to obtain the reference road gradient profiles.

Compared Methods: We compared our proposed road gradient estimation system with the EKF-based method (EKF in short) [7] and Artificial Neural Network-based method (ANN in short) [8] to evaluate the system estimation performance. In EKF, the road gradient is estimated based on vehicle altitude and vehicle driving states (vehicle longitudinal velocity, active gear and engine torque). The above values are obtained as follows: vehicle altitude and longitudinal velocity are measured with the smartphone; the active gear and engine torque are used to calculate the driving torque. However, drivers



(a) Roads for driving experiments (b) Zoomed map of road in red color

Fig. 7. Experimental roads in the urban area of Charlottesville.

adjust active gears frequently in practice and it is difficult to measure active gear in real time. Here we directly calculate the driving torque with vehicle velocity, acceleration and vehicle mass through the driving torque estimation method in [7] to avoid the measurement of active gear and engine torque. EKF also considers the data measurement noise and drift noise during the road gradient estimation process. ANN estimates road gradient using the neural network method based on vehicle related states including velocity, acceleration and altitude. We used total 4,320 samples to train ANN. For each sample, it contains vehicle velocity, acceleration and altitude measured with the smartphone and its corresponding road gradient ground truth at each location.

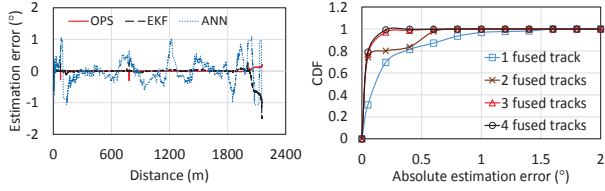
A. Experimental Settings

1) *Road information:* The experimental roads in the area of Charlottesville are total 164.80km long and shown in Figure 7(a). The experimental roads are divided into two parts marked with the red color and the black color. The road marked with red color is used to show the performance of the road gradient estimation system in a small scale and its zoomed map is shown in Figure 7(b). The roads marked with black color is used to verify the proposed system estimation performance and conduct performance comparisons between proposed system and other road gradient estimation methods in a large scale. For the road marked with red color, people can make lane change actions and its road gradient changes frequently, so it can also be used to test the lane change detection algorithm. Here, we discuss our system's estimation performance and make the comparisons with other methods in both small-scale and large-scale road network.

TABLE III
ROAD GRADIENT AND ROAD LANE NUMBERS OF THE ROAD.

Section	0-1	1-2	2-3	3-4	4-5	5-6	6-7
Uphill(+)/downhill(-)	+	-	+	-	+	-	+
The num. of lanes	1	1	1	1	2	2	1

The road marked with red color in Figure 7(a) starts from point 0 to point 7 shown as Figure 7(b). It is total 2.16km long and some parts of the road have one lane while some others have two lanes in the same direction. Therefore, one type is the road with one road line and the other type is the road with two road lanes. As shown in Figure 7(b), the triangle marks separate the road into small sections based on its reference road gradient profile and road types. We use negative road gradients to represent downhill roads and use positive road gradients to represent uphill roads. Table III shows the features of each section of the road.

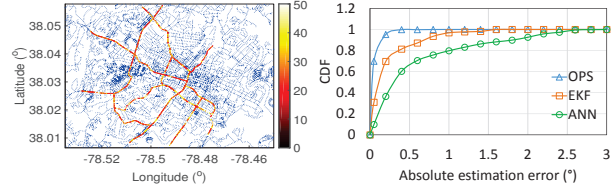


(a) Absolute estimation errors (b) CDFs for different track fusions
Fig. 8. Road grade estimation performance comparisons.

2) *Data collection:* We drove the vehicle on the experiment road to collect data for road gradient estimation accuracy comparisons among EKF, ANN and our system. The data used by EKF includes vehicle altitude, vehicle velocity, and vehicle acceleration. The vehicle altitude was measured through the smartphone built-in barometer. As in [25], [26], the vehicle velocity and the vehicle acceleration were measured with the speedometer and the accelerometer in the smartphone, respectively. For ANN, it needs the data including vehicle velocity, vehicle acceleration and vehicle altitude and these data were measured through the smartphone. For our system, it needs different vehicle velocity profiles and steering rate to estimate road gradients. Vehicle velocity profiles of one vehicle were obtained based on GPS, speedometer, and accelerometer in the smartphone and CAN-bus. Based on different vehicle velocity profiles, our system firstly estimated individual road gradient profiles and then fused the estimated road gradient profiles into one final road gradient profile. The steering rate was calculated based on the method in Section III-A and used to detect lane change actions and adjust vehicle velocity values. To obtain accurate reference road gradient profile with low computation time cost, we set road segment length to 1 meter to calculate the reference profile.

B. Experimental Results

1) *Road gradient estimation performance:* For the driving experiment in Figure 7(b), the road gradient estimation comparisons between our proposed system (OPS), EKF and ANN are conducted. Here, the absolute estimation error is used to describe the road gradient estimation accuracy per each measurement and calculated as the difference between estimated road gradient value and road gradient ground truth value. The absolute estimation error comparisons between OPS, EKF and ANN are shown in Figure 8(a). The value in the x axis represents the vehicle position relevant to the start-point in the experiment. We see that OPS has the least absolute estimation error compared with EKF and ANN, and Mean Relative Errors (MREs) for OPS, EKF and ANN equal to 11.9%, 20.3% and 31.6% respectively, which demonstrates high road gradient estimation accuracy of OPS. This is because OPS eliminates the negative effects of lane change actions on the road gradient estimation and improves the road gradient estimation accuracy by fusing different estimated road gradient tracks. Besides, ANN has larger absolute estimation error than both OPS and EKF. This is because only 4,320 samples are used to train the ANN and these training samples are not enough for ANN, which reduces its estimation accuracy. Though ANN does not



(a) Estimated road gradient (degree) (b) CDFs for different methods
Fig. 9. Road gradient estimation of road network in Charlottesville.

require that the relationship between road gradient and inputs is pre-known, it needs to be trained periodically to update its inertial architectures and its estimation accuracy is affected greatly by the number of training samples, which limits its application in road gradient estimation.

In our proposed system, vehicle velocities from four different sources are used to estimate road gradient. Total four corresponding road gradient tracks are formed and sent to track fusion method for final road gradient estimation. To study how the number of tracks affects road gradient estimation accuracy, we fuse different number of road gradient tracks using the track fusion method to obtain the estimated road values. The Cumulative Distribution Functions (CDFs) of road gradient estimation with different tracks are shown in Figure 8(b). When the value in the y axis equals to 0.5, absolute estimation error for the road gradient estimation with no track fuse is 0.23 and values with track fusion are around 0.09, which demonstrates the effectiveness of track fusion method on improving road gradient estimation accuracy. We also see that the absolute estimation error can be reduced significantly when the number of fused tracks is 3 or more. It helps us to determine how many velocity sensors are needed to ensure high estimation accuracy in practice.

To evaluate the robustness of proposed system on different road conditions (i.e., lane change, out of GPS service), we did the driving experiment on large-scale road network shown in Figure 7(a) and applied our system to estimate their road gradient profiles. The estimated road gradient of road network in Charlottesville is shown in Figure 9(a). The color bar on the right represents different road gradient values; the road with dark red has small road gradient while the road with orange has high road gradient. The reference profiles of such road network are calculated through the method introduced in Section III-D. MRE of road gradient estimation is 12.4% and close to the estimation result in the small-scale road experiment. Therefore, our proposed method has high robustness on different road conditions and can be used to estimate the road gradient for roads where drivers change lanes or GPS service is not available in a city.

CDFs between OPS, EKF and ANN are compared in Figure 9(b). We see that OPS has the least estimation error compared with EKF and ANN. More specifically, when the value in the y axis equals to 0.5, the absolute estimation errors of OPS, EKF and ANN are 0.09, 0.13 and 0.36, respectively. We see that for the same value in the y axis, OPS always has least estimation error compared with EKF and ANN. This is because OPS uses lane change detection to eliminate lane change effects

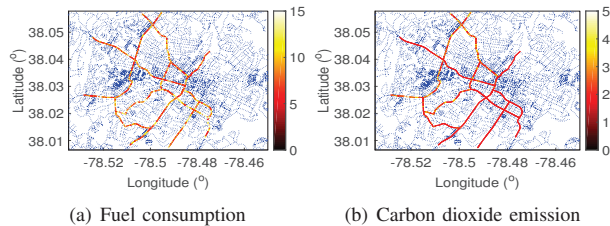


Fig. 10. Vehicle fuel consumption (gallon/hour/vehicle) and pollution emission (ton/km/hour) estimations in Charlottesville.

on estimation accuracy and uses the track fusion algorithm to reduce the effects of sensor measuring noise and drift noise.

C. Application: Fuel Consumption and Pollution Emission Estimations

Based on Section IV-B, we see that our proposed system has high road gradient estimation accuracy. Its estimation results can be applied to real-world services. For example, road gradient affects vehicle fuel consumption and air pollution emission greatly, and accurate road gradient estimation helps to improve vehicle fuel consumption and pollution emission estimation accuracy. For vehicle fuel consumption estimation, we integrated road gradient values into the fuel consumption model and calculated the fuel consumptions when the passenger vehicle drives in the city with average driving speed 40km/h . Figure 10(a) visualizes the average fuel consumptions per hour in the city. By comparing Figure 9(a) and Figure 10(a), we see that high fuel consumption values per hour are always located at road segments with large road gradients, which explains why the vehicle driving on the uphill usually consumes much more fuel compared with that at flat roads. Since Figure 10(a) provides more accurate vehicle fuel consumption by considering the road gradient, it can be applied into vehicle routing plan area to determine the best route to minimize the fuel consumption.

For vehicle pollution emission estimation, we integrated fuel consumption per vehicle with average traffic volume at each road to calculate the average vehicle pollution emission. Here, we got average traffic volumes of streets from Annual Average Daily Traffic [27] and applied them into the vehicle emission model in Section III-E to calculate carbon dioxide emissions shown in Figure 10(b). We see that carbon dioxide emission distribution is different from fuel consumption distribution in Figure 10(a). This is because total carbon dioxide emission for certain road segment is determined by both fuel consumption per vehicle and real-time traffic volume. Real-time estimation on carbon dioxide emission distribution in the urban area is important for the government and can help to control vehicle air pollution emission and monitor air quality.

V. RELATED WORK

Current road gradient estimation methods can be divided into measurement-based methods and algorithm-based methods. Measurement-based methods [9], [10], [11] measure the road gradient through visual inspections or direct measurements of road irregularities with a fully instrumented vehicle. However,

these methods are extremely expensive to implement and have high requirements on sensor accuracy and signal processing speed during the operation. Algorithm-based methods adopt the algorithms such as Extended Kalman Filter, data fusion and Artificial Neural Network [8], [5], [6], [7] to estimate the road gradient based on measured vehicle states. Compared with measurement-based methods, algorithm-based methods are inexpensive to implement. However, these methods have relatively low estimation accuracy and are conducted with special assumptions on vehicle parameters, which may be difficult to obtain. Besides, they ignore the effect of individual driving actions such as lane change on road gradient estimation. Our method estimates road gradient with only smartphones. Besides, we build lane change detection algorithm to eliminate the negative effects of lane change.

Many efforts have been made to exploit the smartphone application in vehicle steering behavior detection. Current smartphone based steering behavior detection methods can be divided into smartphone camera-based methods and smartphone camera-free methods. For smartphone camera-based methods [28], [29], [30], the image of vehicle position with respect to the lane boundaries are captured and then analyzed with imaging processing to detect vehicle steering actions. However, these methods have high requirements on clear road view and good light condition and high computation load can easily run out of the smartphone energy. Smartphone camera-free methods [31], [32], [18] take full advantages of in-built sensors to describe vehicle steering behavior and detect steering behavior types. However, these methods only discussed how to detect lane change actions based on smartphone sensors but did not discuss possible effects of lane change actions on road gradient estimation accuracy and how to eliminate their effects. Our proposed lane change detection method considers the effects of lane change actions and eliminates their effects by adjusting vehicle states.

Several existing fuel consumption and emission estimation methods have been proposed to estimate vehicle fuel consumption and pollution emission. One group of works [33], [34], [35] conduct estimation based on empirical relationships between fuel consumption and vehicle states such as velocity and acceleration. Another group of works [36], [37], [38] estimate fuel consumption and pollution emission based on vehicle driving equation which describes the power needed under different speeds and accelerations. However, all the above methods do not consider the effect of road gradient on the energy consumption and pollution emission, which can lead to large estimation error for the vehicles driving on the road with large road gradients. In this paper, we utilize the road gradient estimation system to estimate road gradient and integrate road gradient values into fuel consumption and pollution emission models to obtain more accurate fuel consumption and pollution emission estimation.

VI. CONCLUSION

In this paper, we infer the road gradient of a city's road network based on measured vehicle driving states. However, it

is a challenge to estimate road gradient with high accuracy and implementation convenience. To overcome this challenge, we proposed a road gradient estimation system which estimates the road gradient with only smartphone. In the proposed system, we firstly designed a lane change detection algorithm to eliminate the negative influences of lane changes. Then, we built the vehicle state space equation and applied EKF and the track fusion algorithm to estimate road gradient and also improve estimation accuracy. Finally, we conducted driving experiments in the Charlottesville city to evaluate our system. The results demonstrate that our method has high estimation accuracy and the road gradient estimation error can be reduced by 22% compared with other methods. We also applied road gradient values into the fuel consumption and pollution emission model to obtain more accurate estimation of fuel consumption and pollution emission in Charlottesville.

VII. ACKNOWLEDGEMENTS

This research was supported in part by U.S. NSF grants NSF-1827674, CCF-1822965, OAC-1724845, ACI-1719397 and CNS-1733596, and Microsoft Research Faculty Fellowship 8300751.

REFERENCES

- [1] Y. Zheng, L. Capra, O. Wolfson, and H. Yang, "Urban computing: concepts, methodologies, and applications," *ACM Transactions on Intelligent Systems and Technology (TIST)*, vol. 5, no. 3, p. 38, 2014.
- [2] H. C. Frey, K. Zhang, and N. M. Rouphail, "Fuel use and emissions comparisons for alternative routes, time of day, road grade, and vehicles based on in-use measurements," *Environmental Science & Technology*, vol. 42, no. 7, pp. 2483–2489, 2008.
- [3] K. Boriboonsomsin and M. Barth, "Impacts of road grade on fuel consumption and carbon dioxide emissions evidenced by use of advanced navigation systems," *Transportation Research Record: Journal of the Transportation Research Board*, no. 2139, pp. 21–30, 2009.
- [4] G. Map, "Google map adds elevation profiles to bike routes to help you avoid those steep hills," <https://www.engadget.com/2014/05/17/google-maps-bike-route-elevation-data/>, 2016.
- [5] E. J. Holm, "Vehicle mass and road grade estimation using kalman filter," *Dissertation, Linköping University, Sweden*, 2011.
- [6] H. Jansson, E. Kozica, P. Sahlholm, and K. H. Johansson, "Improved road grade estimation using sensor fusion," in *Proc. of the 12th Reglermöte in Stockholm, Sweden*. Citeseer, 2006.
- [7] P. Sahlholm and K. H. Johansson, "Road grade estimation for look-ahead vehicle control using multiple measurement runs," *Control Engineering Practice*, vol. 18, no. 11, pp. 1328–1341, 2010.
- [8] H. M. Ngwangwa, P. S. Heyns, F. Labuschagne, and G. K. Kululanga, "Reconstruction of road defects and road roughness classification using vehicle responses with artificial neural networks simulation," *Journal of Terramechanics*, vol. 47, no. 2, pp. 97–111, 2010.
- [9] H.-J. Kim, H. S. Yang, and Y.-P. Park, "Improving the vehicle performance with active suspension using road-sensing algorithm," *Computers & Structures*, vol. 80, no. 18, pp. 1569–1577, 2002.
- [10] J. S. Dyer, S. A. Dyer, D. D. Day, and J. J. Devore, "On a simple method for estimating international roughness index using a profilograph," in *Proc. of IMTC*. IEEE, 2008, pp. 1526–1530.
- [11] D. Chen, D.-H. Chen, J.-R. Chang, and K.-T. Chang, "Application of 3d laser scanning on measuring pavement roughness," *Journal of Testing and Evaluation*, vol. 34, no. 2, pp. 1–9, 2005.
- [12] J. Dong, D. Zhuang, Y. Huang, and J. Fu, "Advances in multi-sensor data fusion: Algorithms and applications," *Sensors*, vol. 9, no. 10, pp. 7771–7784, 2009.
- [13] T. Hao, "A smartphone system for unobstructive personal living routine monitoring," in *Proc. of SenSys*, 2013.
- [14] J. Paefgen and F. Kehr, "Driving behavior analysis with smartphones: insights from a controlled field study," in *Proc. of MUM*, 2012.
- [15] S. E. Lee, E. C. Olsen, and W. W. Wierwille, "A comprehensive examination of naturalistic lane-changes," Tech. Rep. No. HS-809 702, 2004.
- [16] C. Loader, *Local regression and likelihood*. Springer Science & Business Media, 2006.
- [17] A. M. C. Odhams, "Identification of driver steering and speed control," Ph.D. dissertation, University of Cambridge, 2007.
- [18] D. Chen, K.-T. Cho, S. Han, Z. Jin, and K. G. Shin, "Invisible sensing of vehicle steering with smartphones," in *Proc. of International Conference on Mobile Systems, Applications, and Services*, 2015, pp. 1–13.
- [19] G. Liu, M. Iwai, Y. Tobe, D. Matekenya, K. M. A. Hossain, M. Ito, and K. Sezaki, "Beyond horizontal location context: measuring elevation using smartphone's barometer," in *Proc. of ACM International Joint Conference on Pervasive and Ubiquitous Computing: Adjunct Publication*, 2014, pp. 459–468.
- [20] E. Ozatay, S. Onori, J. Wollaeger, U. Ozguner, G. Rizzoni, D. Filev, J. Michelini, and S. Di Cairano, "Cloud-based velocity profile optimization for everyday driving: A dynamic-programming-based solution," *IEEE Transactions on Intelligent Transportation Systems*, vol. 15, no. 6, pp. 2491–2505, 2014.
- [21] P. Sahlholm and K. H. Johansson, "Road grade estimation for look-ahead vehicle control," *IFAC Proceedings Volumes*, vol. 41, no. 2, pp. 3380–3385, 2008.
- [22] S. Haykin and O. Hamilton, *Kalman filtering and neural networks*. Wiley Online Library, 2001.
- [23] C.-Y. Chong, S. Mori, W. H. Barker, and K.-C. Chang, "Architectures and algorithms for track association and fusion," *IEEE Aerospace and Electronic Systems Magazine*, vol. 15, no. 1, pp. 5–13, 2000.
- [24] K. M. Sentoff, L. Aultman-Hall, and B. A. Holmén, "Implications of driving style and road grade for accurate vehicle activity data and emissions estimates," *Transportation Research Part D: Transport and Environment*, vol. 35, pp. 175–188, 2015.
- [25] B. Liu, N. Liu, G. Chen, X. Dai, and M. Liu, "A low-cost vehicle anti-theft system using obsolete smartphone," *Mobile Information Systems*, 2018.
- [26] Y. Gu, Q. Wang, and S. Kamijo, "Intelligent driving data recorder in smartphone using deep neural network-based speedometer and scene understanding," *IEEE Sensors Journal*, 2019.
- [27] "Virginia department of transportation," <http://www.virginiadot.org/info/ct-trafficcounts.asp>, 2017.
- [28] W. Liu, X. Wen, B. Duan, H. Yuan, and N. Wang, "Rear vehicle detection and tracking for lane change assist," in *Proc. of Intelligent Vehicles Symposium*. IEEE, 2007, pp. 252–257.
- [29] B. Morris, A. Doshi, and M. Trivedi, "Lane change intent prediction for driver assistance: On-road design and evaluation," in *Proc. of Intelligent Vehicles Symposium (IV)*. IEEE, 2011, pp. 895–901.
- [30] S.-Y. Chen and J.-W. Hsieh, "Edge-based lane change detection and its application to suspicious driving behavior analysis," in *Proc. of IJHMSP 2007*, vol. 2. IEEE, 2007, pp. 415–418.
- [31] J. F. Júnior, E. Carvalho, B. V. Ferreira, C. de Souza, Y. Suhara, A. Pentland, and G. Pessin, "Driver behavior profiling: An investigation with different smartphone sensors and machine learning," *PLoS one*, vol. 12, no. 4, p. e0174959, 2017.
- [32] D. A. Johnson and M. M. Trivedi, "Driving style recognition using a smartphone as a sensor platform," in *Proc. of Intelligent Transportation Systems (ITSC)*. IEEE, 2011, pp. 1609–1615.
- [33] L. I. Panis, S. Broekx, and R. Liu, "Modelling instantaneous traffic emission and the influence of traffic speed limits," *Science of the total environment*, vol. 371, no. 1, pp. 270–285, 2006.
- [34] R. Smit, L. Ntziachristos, and P. Boulter, "Validation of road vehicle and traffic emission models—a review and meta-analysis," *Atmospheric environment*, vol. 44, no. 25, pp. 2943–2953, 2010.
- [35] C. Qiu, H. Shen, A. Sarker, V. Soundararaj, M. Devine, and E. Ford, "Towards green transportation: Fast vehicle velocity optimization for fuel efficiency," in *Proc. of CloudCom*, 2016.
- [36] L. Kang, H. Shen, and A. Sarker, "Velocity optimization of pure electric vehicles with traffic dynamics consideration," in *Proc. of ICDCS*, 2017.
- [37] D. W. Wyatt, H. Li, and J. E. Tate, "The impact of road grade on carbon dioxide (co₂) emission of a passenger vehicle in real-world driving," *Transportation Research Part D: Transport and Environment*, vol. 32, pp. 160–170, 2014.
- [38] J. L. Jimenez-Palacios, "Understanding and quantifying motor vehicle emissions with vehicle specific power and tildas remote sensing," Ph.D. dissertation, Massachusetts Institute of Technology, 1998.